



An Analysis of Boundary Layer Moistening Process of Three MJO events during DYNAMO IOP

Kai-Chih Tseng and Chung-Hsiung Sui

Department of Atmospheric Sciences, National Taiwan University, Taipei, Taiwan, 106

1. Introduction

➤ Previous Work

- Based on Hsu et al.(2012), boundary layer asymmetric moistening causes MJO eastward propagation.
- Kuang (2008) used cloud system resolving model with large-scale prescribed gravity wave successfully simulated convective coupled wave.
- Lau et al. (2010) found warm rain process with low-level adiabatic heating in the build-up phase of MJO, supporting a pre-moistening condition

➤ Scientific issues:

- What is the main mechanism causes pre-moistening condition?
- Is shallow convection existing in reanalysis data?
- Can we use reanalysis data comparing with field observation or satellite data?

2. Data and Method

We use scale-separation to diagnose boundary moistening process. All variables here are separated into three different time scales (1)over 60 days (low-frequency) (2)20 to 60 days (MJO-filtered) (3)below 20 days (synoptic scale) and residual term. Domain selection is based on DYNAMO field observation array. The collective effect of eddy activities is estimated by a moisture budget residual. Yanai et al.(1973). To examine whether reanalysis data is reliable, we adopt TRMM data to examine the relationship between reflectivity(2A23) and Q2(EC-Interim) vertical profile in the second part of result. Data information is available in table 1. TRMM 2A23 are back to the same Nadir every 12 hours and we take daily average as our unit time step. For 3B42 data and EC-Interim, we take six hours as unit time step and diagnose with domain average (70E~80E, 5S~5N). Both 2A23 and 2A25 are selected with value passing statistical significance. (undefined value such as -9999→not detected, -8888→no rain, -1111→low level confidence are removed)

Moisture budget

Yanai et al. (1973)

$$\frac{\partial q}{\partial t} = -V \cdot \nabla q - \omega \frac{\partial q}{\partial p} + e - c$$

condensation (e - c)

evaporation (e - c)

$$\frac{\partial q}{\partial t} = -(V_{20} + V_{20-60} + V_{60}) \cdot \nabla (q_{20} + q_{20-60} + q_{60}) - (\omega_{20} + \omega_{20-60} + \omega_{60}) \frac{\partial}{\partial p} (q_{20} + q_{20-60} + q_{60})$$

Resolved scale

$$+ e - c - V' \cdot \nabla q' - \omega' \frac{\partial q'}{\partial p}$$

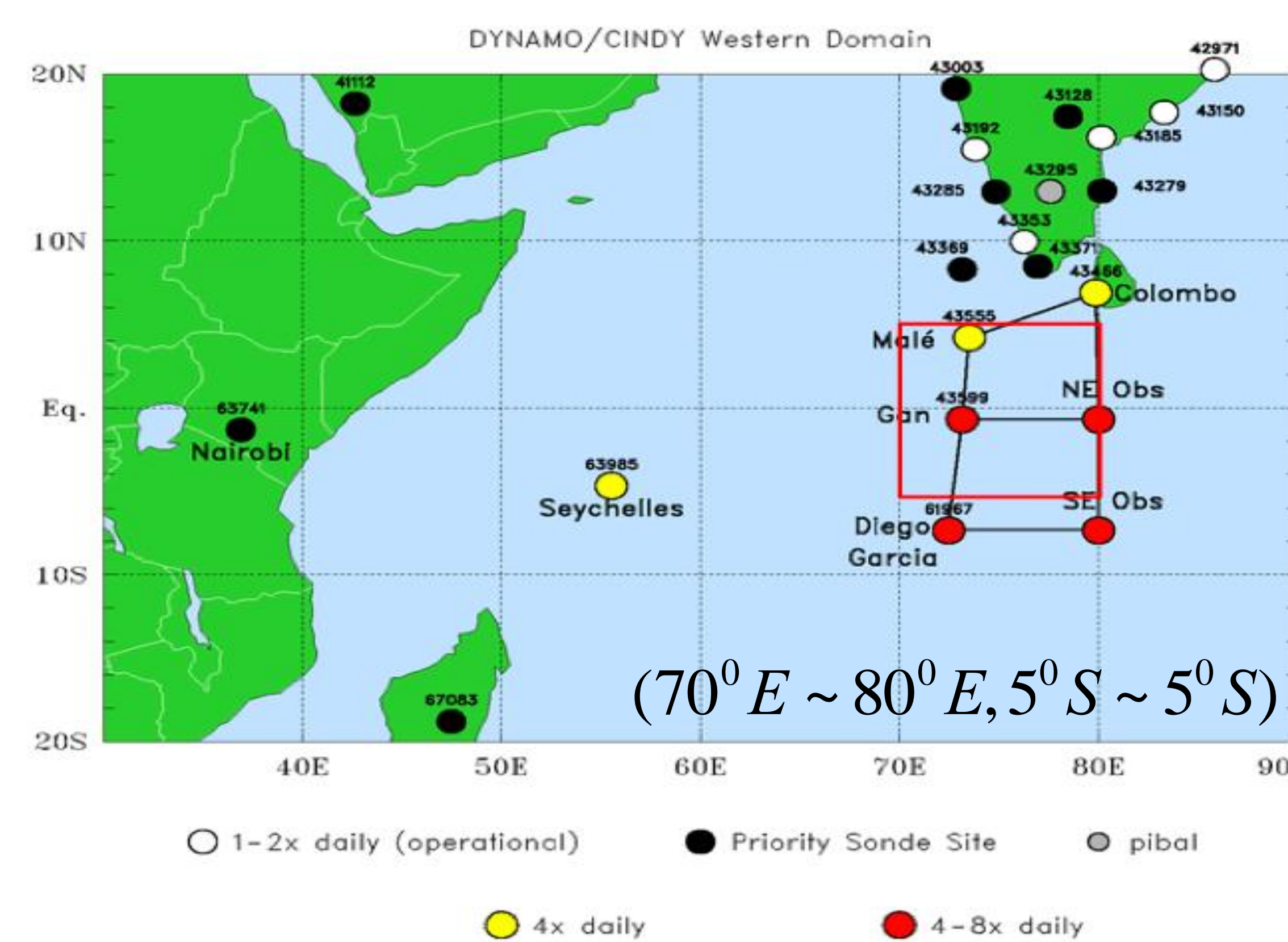
Unbalanced residual term

Convective eddies

where $-\frac{Q_2}{L} = e - c - V' \cdot \nabla q' - \omega' \frac{\partial q'}{\partial p}$

Domain Selection

<http://johnson.atmos.colostate.edu/dynamo/>



Data description

Table 1

	Horizontal resolution	Time resolution	Available period
Storm Height (2A23) and Reflectivity(2A25)	5.0*5.0 km ²	~12 hr (back to the same Nadir)	2001-08-24 ~now
Rain Rate(3B42)	0.25° *0.25° (lat*lon)	3hr	1998-01-01 ~now
ECMWF-Interim	0.75°*0.75° (lat*lon)	6hr	1979~now

3. Result(1)---moisture budget

Our result reveals that dominant balance of boundary moisture budget comes from synoptic scale vertical advection and eddies activity which represents the importance of convective eddies and convective couple wave.(Fig 1 & Fig2) In Fig 1, we use whisker box present the variation of all variables in the moisture budget and it clearly shows that mean state moisture advection driven by synoptic-scale vertical motion and Q2 have largest variation in these three months. On the other hand, most of horizontal advection are negligible not only mean value but also variations. The low frequency vertical advection of moisture is a prolonged positive term in this season while its time evolution in intraseasonal scale isn't clear enough that may not contribute to intraseasonal variation. Fig2 is the boundary layer integration of dominant term in suppressed of 3 MJO events and it obvious showed that Q2 drives boundary layer moistening process. After suppressed phase, we can identify a steady increasing MJO-filtered moisture vertical advection gets stronger and this is possibly related to MJO convection induced boundary layer convergence. (Hsu et al 2012)

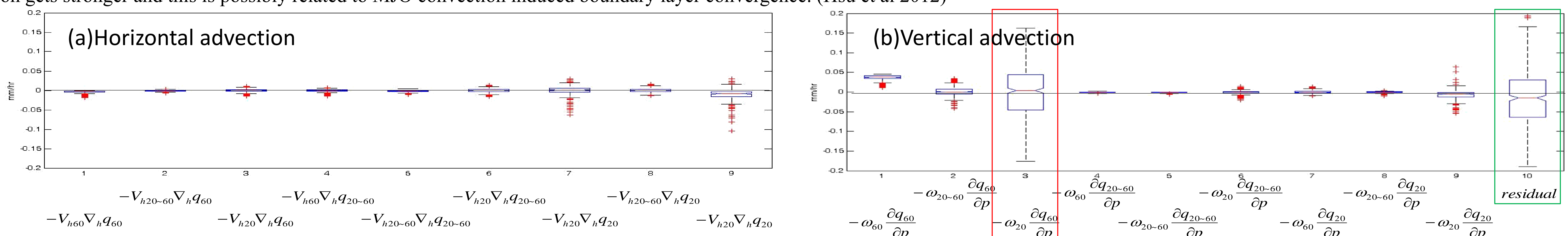


Fig1 Whisker Box (a)horizontal advection (b)vertical advection integrated moisture budget terms in the boundary layer for 3-month IOP.

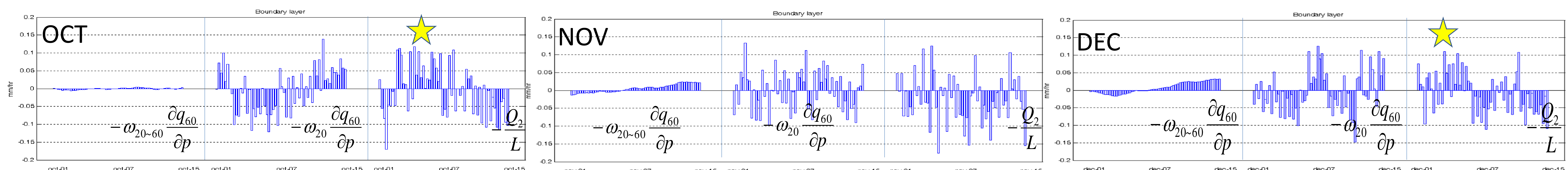


Fig2. Dominant terms boundary integration (1000hPa~850hPa) of first 15 days before convective phase

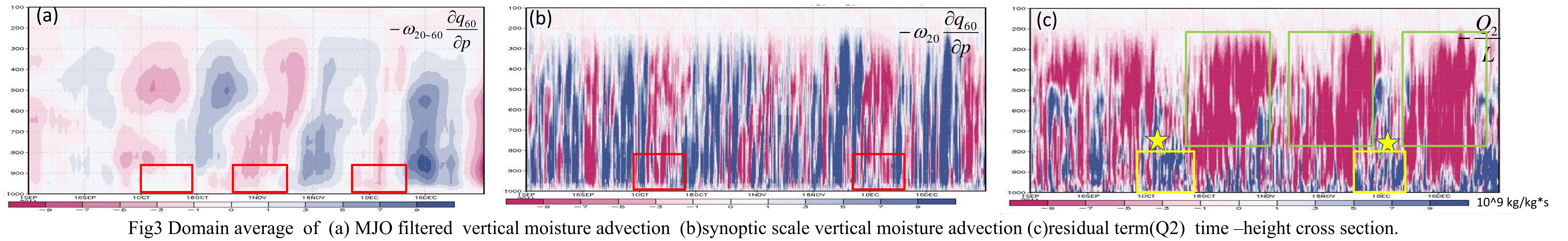


Fig3 Domain average of (a) MJO filtered vertical moisture advection (b) synoptic scale vertical moisture advection (c) residual term (Q_2) time–height cross section.

Fig 3 is time-height cross section of dominant term domain average. In fig 3a 3b and 3c, we can observe vertical tilting structure which boundary layer process is leading free troposphere which also implies the important role of boundary on MJO initiation and propagation. During suppressed phase of these three events, MJO-filtered and synoptic scale subsidence bring dry air from free troposphere (red box) while Q_2 drives moistening which upper boundary is located in 800hPa~850hPa (yellow box marked with star in Fig 3c). In convective phase, positive Q_2 represents the moisture sink related to strong precipitation process (green box).

3. Result(2)---Temporal resolution of cloud joint probability density function

Fig 4 shows cloud transient in different MJO phases by plotting joint probability density function of reflectivity and storm height. In the first five days of October and November, sounding array precipitation is modulated by ITCZ and we can observe intensive frequency around 5km and storm height grows as reflectivity gets stronger which is the characteristic of deep convection. In Oct 06~10, Nov 11~15 and Dec 01~05, the maximum population is concentrated in lower troposphere (<3km) with low reflectivity which implies warm rain process during suppressed phase and this result lined with Q_2 vertical profile that negative Q_2 near surface may result from convective eddies while local maximum located in the top of boundary is the symbol of shallow convection. In the next five days after suppressed phase (October 11~15, November 16~20 and December 05~10) are transient phase mixed with shallow cloud and increasing congestus. The following convective phase, abundant congestus and deep convection consists Q_2 vertical profile which local maximum is located in 500hPa and this represents the moisture sinking related to strong precipitation.

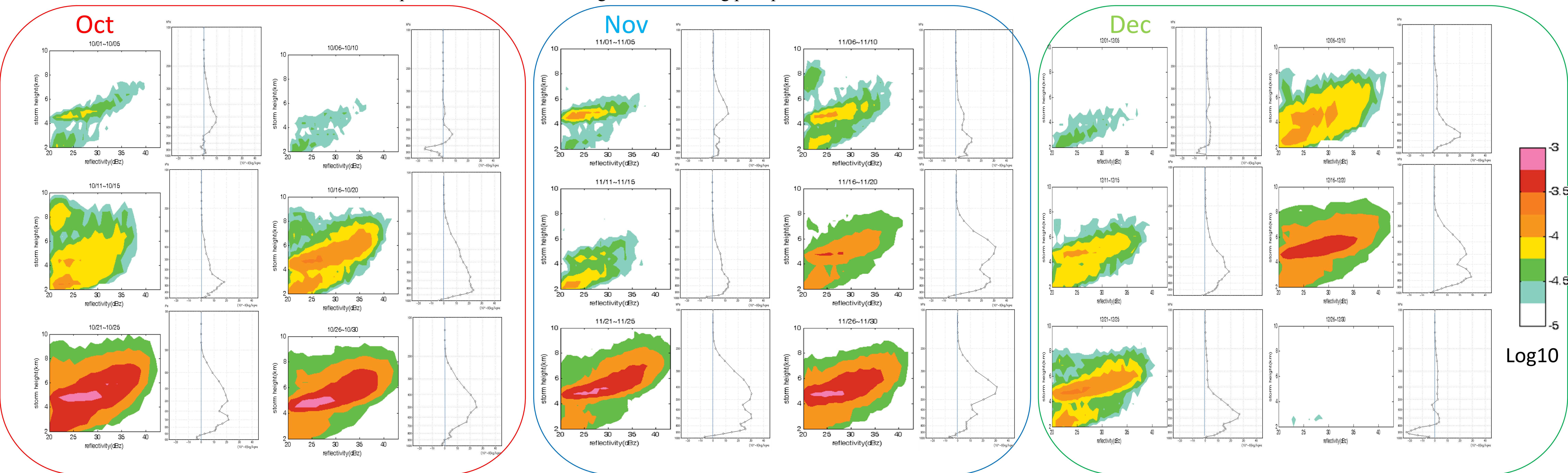


Fig 4 Every five-day joint probability density function of cloud (storm height and reflectivity) in DYNAMO IOP and shading represents occurrence frequency with log coordinate. (left column) The right hand side column represent Q_2/L vertical profile of five-day and domain average with unit 10^{-9} kg/kg*s.

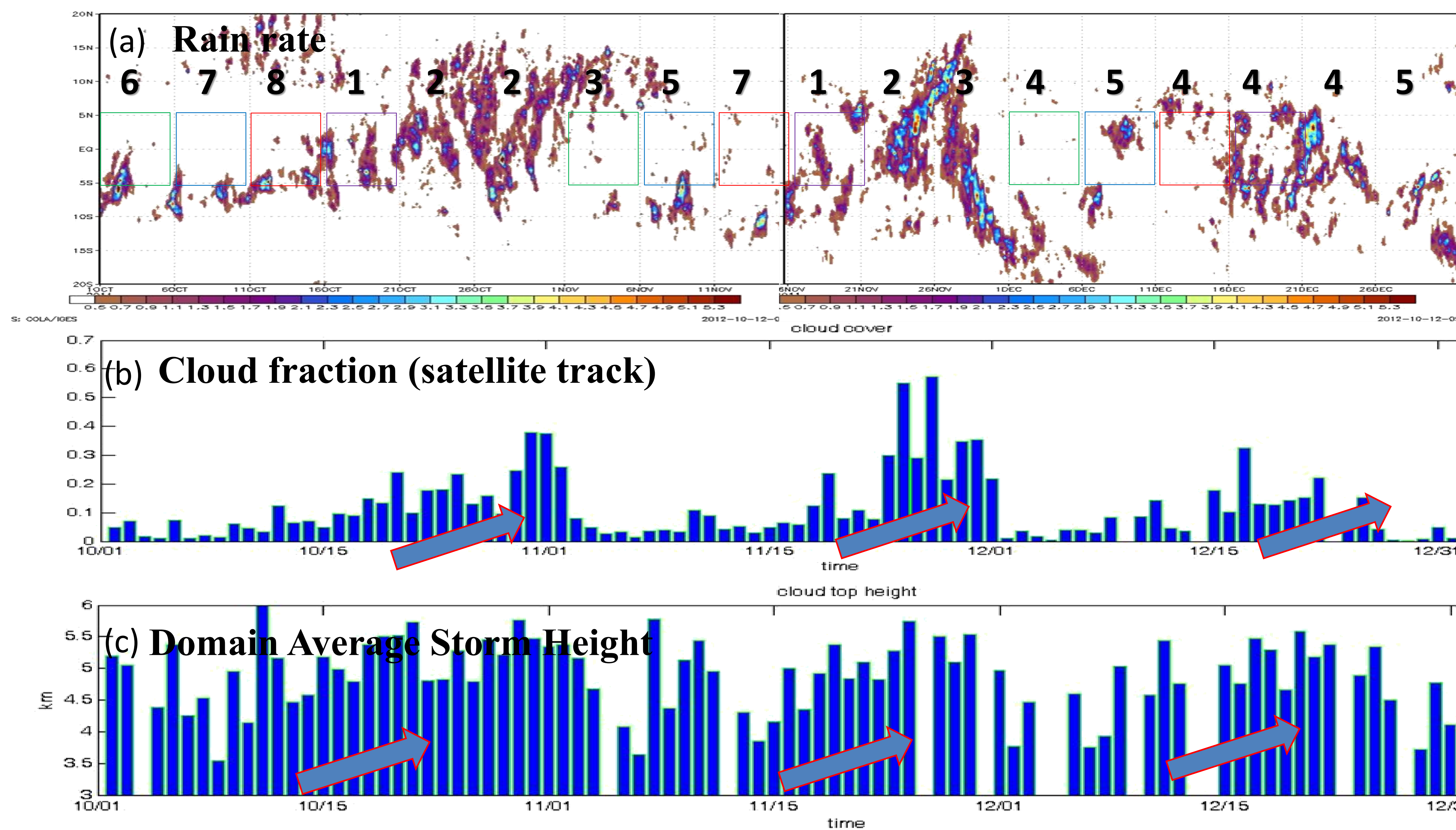


Fig 5 (a) precipitation rate from 3B42 (b) cloud fraction in the domain derived by integrating probability density function in figure 4 (2A23 storm height data) (c) Domain average storm height with unit km. The number in (a) is MJO RMM index (Wheeler and Hendon 2004)

6. Conclusion

The MJO events in DYNAMO show a clear evolution through suppressed, transition and convective stages

- The synoptic-scale vertical advection and Q_2 dominate the column moisture budget.
- During the suppressed phase, eddy activities moisten boundary layer (negative Q_2) while synoptic scale downward motion from free troposphere dries it.
- TRMM 2A23 and 2A25 show an evolution from abundant shallow (<3km) clouds in the suppressed phase, to the transition phase populated by both shallow clouds and congestus clouds, and finally to the convective phase with more congestus and deep convection developed.

Reference

1. Hsu, P.-C., and T. Li, 2012: Role of the boundary layer moisture asymmetry in causing the eastward propagation of the Madden–Julian oscillation. *J. Climate*, **25**, 4914–4931
2. Lau, K.-M., and H.-T. Wu, 2010: Characteristics of Precipitation, Cloud, and Latent Heating Associated with the Madden–Julian Oscillation. *J. Climate*, **23**, 504–518.
3. Yanai, M., S. Esbensen, and J.-H. Chu, 1973: Determination of bulk properties of tropical cluster from large-scale heat and moisture budget. *J. Atmos. Sci.*, **30**, 611–627